Applied Surface Science 311 (2014) 503–507

Contents lists available at ScienceDirect

Applied Surface Science

journal homepage: www.elsevier.com/locate/apsusc

Electrical and magnetic effect of transition metals in SnSb nanoalloy

P. Nithyadharseni[a], B. Nalini[b,*], P. Saravanan[c]

[a] Department of Physics, Karunya University, Karunya Nagar, Coimbatore 641014, India
[b] Department of Physics, Avinashilingam University, Coimbatore, India
[c] Defence Metallurgical Research Laboratory, Hyderabad 500058, India

ARTICLE INFO

Article history:
Received 5 December 2011
Received in revised form 12 May 2014
Accepted 14 May 2014
Available online 27 May 2014

Keywords:
SnSb alloy
Nanostructured materials
Magnetic measurements
Precipitation
Electrical transport
Transition metals

ABSTRACT

Influence of incorporating transition metal impurities such as Fe, Co and Ni on the magnetic and electrical properties of SnSb alloy nanopowders synthesized by reductive co-precipitation is reported. Structural elucidation of all the samples by X-ray diffraction (XRD) confirms hexagonal structure and the morphological observations through scanning electron microscope (SEM) show a minimal particle size of 20 nm for the Co substituted SnSb sample, among all the other impurity incorporated samples. Compositional confirmation of Sn, Sb, Fe, Co, and Ni was made using EDAX. The X-ray photoelectron spectroscopy (XPS) is used to investigate the surface of SnSb and the change in surface activity due to the addition of transition metal impurities. The magnetic hysteresis studies indicate that SnSb and SnSb:Ni exhibit diamagnetic behaviour; while the Fe and Co incorporation resulted in ferromagnetic nature. The conductivity of SnSb:Fe, SnSb:Ni shows a semiconducting nature with negative temperature coefficient of resistance; whereas pure and Co substitution exhibit metallic behaviour with positive temperature coefficient of resistance. The switching of metallic to semiconducting regime is explained in this paper. Also an attempt has been made to correlate electrical and magnetic properties with the surface oxidation effect through XPS data.

1. Introduction

The design, synthesis and characterization of nanophase materials are the subject of intense current research [1]. This activity has been inspired by the realization of the physical and chemical properties of nanophase materials that are dramatically different from those of the bulk counterparts and that nanophase materials often exhibit new phenomena. Magnetic particles, for example, exhibit size effects. Below a critical size, magnetic nanoparticles become single domain as opposed to multidomain in the bulk structure. Because of their unique physical property of superparamagnetism due to size reduction, magnetic nanoparticles have high potential applications [2].

The present contribution concerns with magnetic and electrical properties of transition metals (Fe, Co and Ni) substituted SnSb nanoalloys. Heringhaus et al. [3] have reported that, the magnetoresistivity of Sn increases strongly when being alloyed with Sb (95Sn-5Sb). On the other hand, studies on the magnetic and electrical behaviour of transition metal impurities like Mn, Fe and Gd in the host material GaSb are reported [4–6]. This makes GaSb compatible with the existing III-V technology. The typical acceptor concentration is $\sim 10^{17}$ cm^{-3} and the acceptors are associated with native Ga vacancy and/or Ga on Sb site defects. The whole concentration is affected when impurity is diffused into GaSb lattice. Also Walle et al. [7] reported that, $AuMnSn_{1-x}Sb_x$ phase exhibits soft ferromagnetism at low temperatures. The paper converges to the fact that the electronic band structure of the $AuMnSn_{1-x}Sb_x$ phase can be calculated, viz., the changes imposed on the electronic band structure and physical properties by the gradual increase in the number of valence electrons on increasing x. Xuan et al. [8] reported that the low-field magnetic entropy changes (ΔS) in $Ni_{43}Mn_{46}Sn_{11-x}Sb_x$ alloys, possessing adjustable martensitic transformation with increase in Sb content, qualifying this material for low cost magnetic refrigeration. Recently, SnSb alloy has picked up interest among the researchers as novel alloy to be employed as negative electrode in lithium ion batteries [9,10]. To the best of our knowledge, studies on the magnetic properties of these Fe, Co and Ni substituted Sn–Sb nanoalloys in the reported compositions is very few; except for the above quoted papers and especially no report on the conductivity properties (AC impedance) of transition metal impurities (Fe, Co and Ni) incorporated SnSb nanoparticles.

Hence the present study explores the magnetic, electrical properties and the compositional analysis of transition metals (Fe, Co

* Corresponding author. Tel.: +91 94862 43092.
E-mail addresses: lalin99@rediffmail.com, nithyadharseni@gmail.com (B. Nalini).

http://dx.doi.org/10.1016/j.apsusc.2014.05.098
0169-4332/

and Ni) substituted SnSb nanoalloys are synthesized by reductive co-precipitation method. The effect due to the addition of transition metal impurities is also explored.

2. Experimental procedure

2.1. Preparation of SnSb alloy nanoparticles

Two aqueous solutions were prepared with appropriate gram molecular weights for the synthesis of SnSb powder, namely solution **1** formed by $SnCl_2{\cdot}2H_2O$, $SbCl_3{\cdot}H_2O$ and sodium citrates; and solution **2** constituted of NaOH and $NaBH_4$ [11] (all the chemicals were AR grade – Merck). The two solutions were mixed together to obtain the required concentration of the SnSb alloy. The precipitates thus obtained were filtered and subsequently washed with distilled water, 0.35 M HCl, and acetone until chlorine was completely washed off and dried at ambient temperature.

2.2. Preparation of transition metals substituted SnSb nanoalloy

The transition metal elements, Fe, Co and Ni, were substituted in excess by 1 g molecular weight of the $FeCl_4$, $CoCl_2$ and $NiCl_2$ in solution 1 and the reductive precipitation was carried out similar to the procedure stated above resulting in the respectively SnSb alloys.

The structure and particle morphologies of synthesized SnSb powder were characterized by X-ray diffraction (XRD – Shimadzu 6000) and scanning electron microscopy (SEM, JEOL 6390)

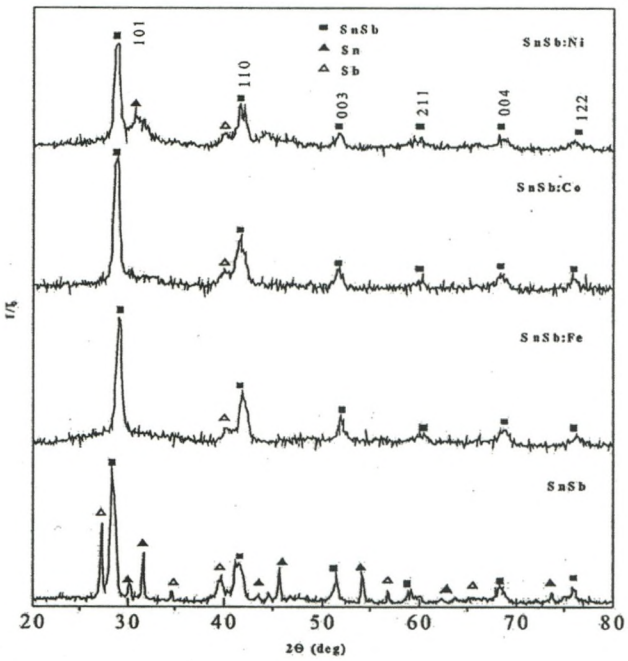

Fig. 1. XRD spectra for SnSb, SnSb:Fe, SnSb:Co and SnSb:Ni samples.

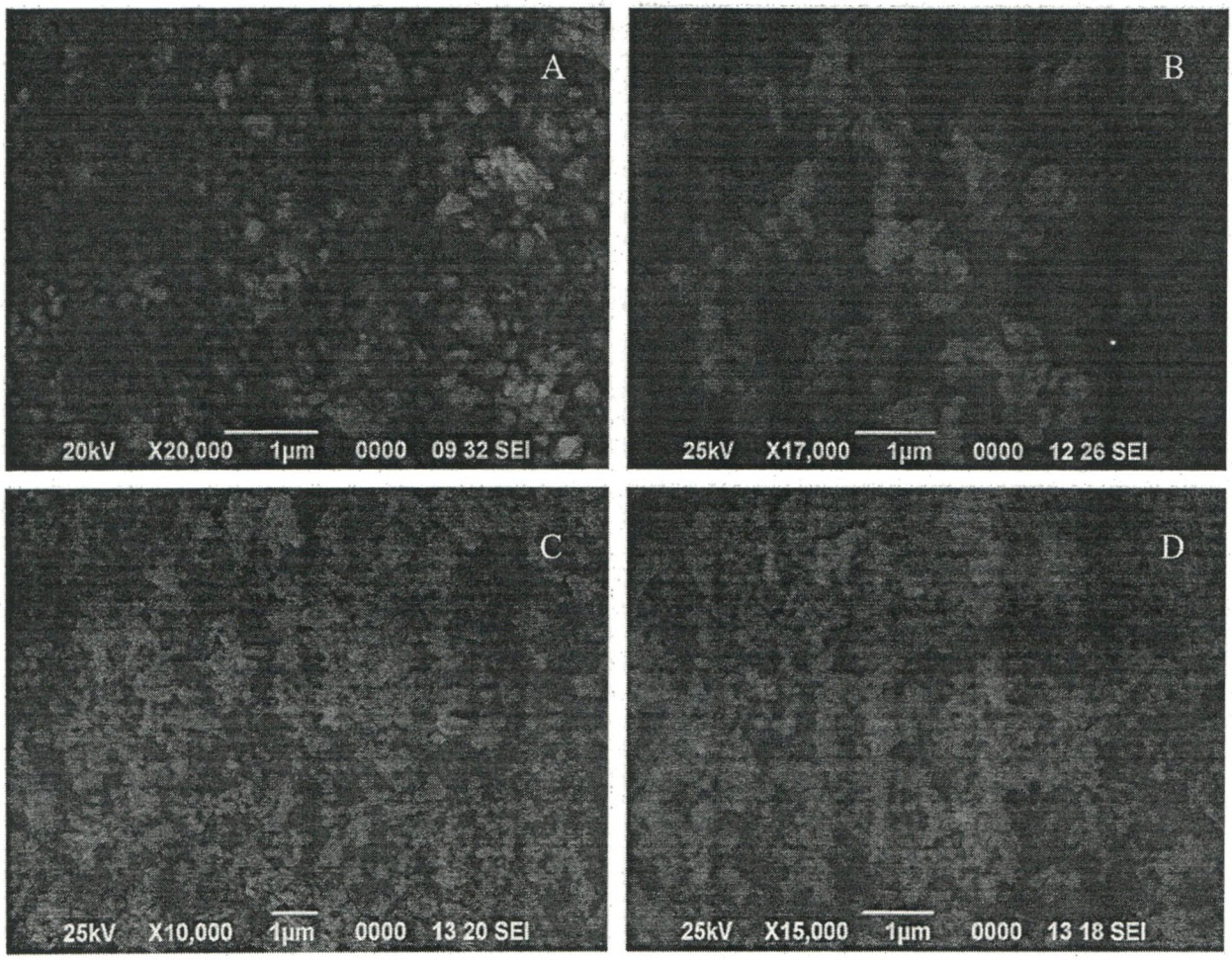

Fig. 2. SEM images of SnSb, SnSb:Fe, SnSb:Co and SnSb:Ni samples.

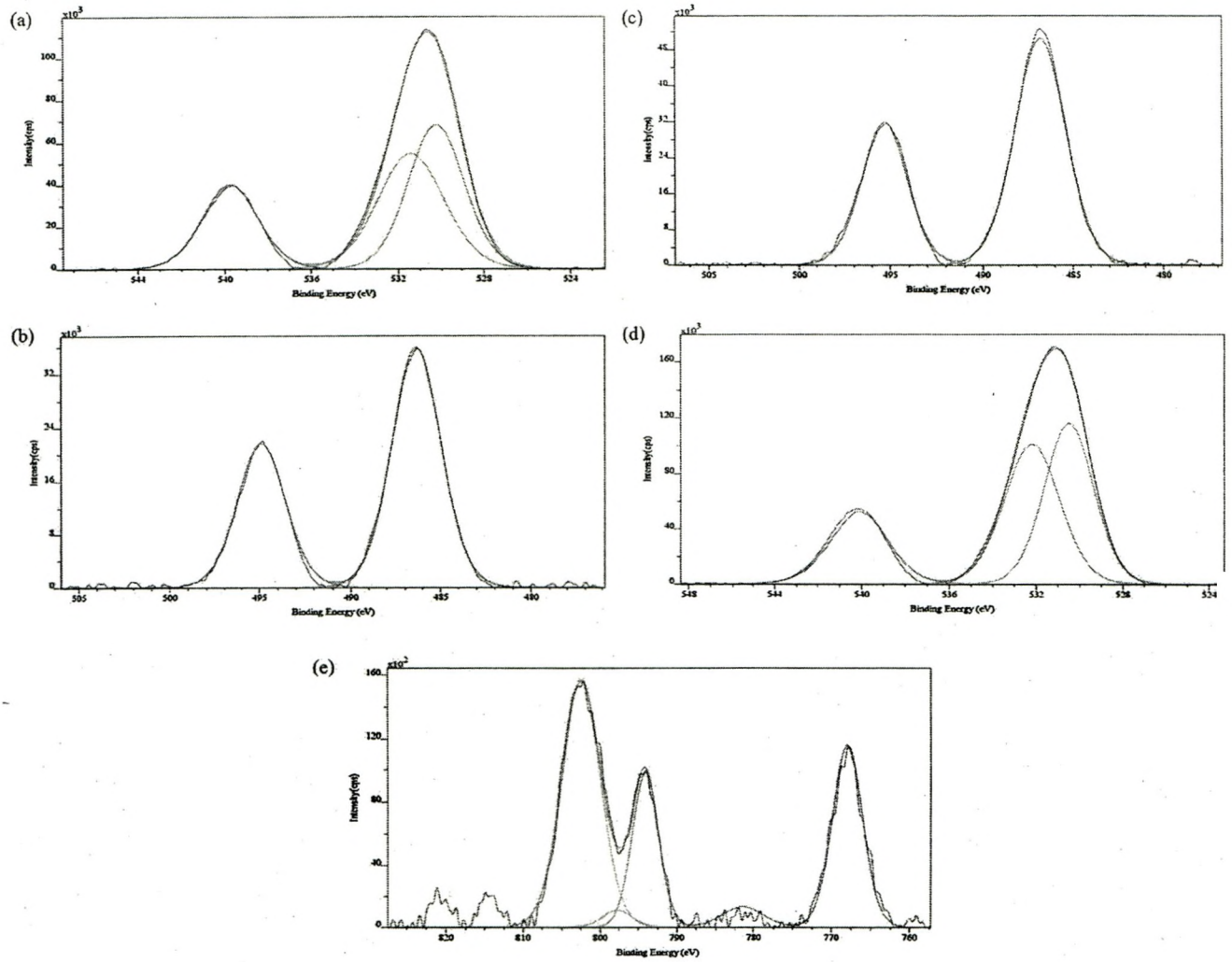

Fig. 3. XPS spectra for (a and b) SnSb and SnSb:Co samples at Sb 3d, (c and d) SnSb and SnSb:Co samples at Sn 3d, (e) SnSb:Co sample at Co 2p.

respectively. Elemental analysis was carried out with energy dispersive X-ray analysis spectrum (EDAX, Oxford INCA Energy MnK_α – 137 eV) and magnetic properties were studied using vibrating sample magnetometer (VSM, Lakeshore 7407). The surface chemical compositions of prepared alloys were analyzed by X-ray photoelectron spectroscopy (XPS). A standard MgK_α excitation source (1253.6 eV) was employed. The binding energy (BE) scale was calibrated by measuring the reference peak of C1s (BE = 284.6 eV) [12] from the surface contamination. In order to measure the electrical properties of the samples, silver foil was glued on either face of the sample to serve as electrode. Electrical impedance (Z), phase angle (θ), conductivity were measured as a function of frequency (1 Hz–100 kHz) at different temperatures using a computer controlled LCR Hi-Tester (HIOKI 3532). To overcome the effect of moisture, if any, on electrical properties, the samples were sintered to 250 °C for 2 h and then cooled to room temperature prior to the measurements. All the impedance Nyquist plots were fitted using Zview software and the equivalent circuits were analyzed.

3. Results and discussion

Fig. 1 shows the XRD pattern for the SnSb, SnSb:Fe, SnSb:Co and SnSb:Ni alloy nanoparticles respectively. Size reduction of crystallites (as calculated from Debye Scherrer formula) from 18 nm in pure and Fe substituted SnSb to 11 nm in Co sample brings forth a peak broadening in XRD pattern of the later sample. No evidence of discrete oxide peaks is observed in all the samples as the transition elements are prone for oxidation in wet chemical route. The peaks are assigned to hexagonal structure (β-SnSb phase (JCPDS #33-0118), which belongs to the space group R-3m (166)) that matches well with nearly same d-values. Though, Park et al. [13], have reported that SnSb exists in rhombohedral structure at a different stoichiometry of Sn and Sb, the samples prepared in this work is hexagonal. Rhombohedral is a special case of hexagonal, if $-h+k+l=3n$ (where h, k, l are miller indices and n is an integer). Analysis of all the samples could be assigned with *hkl* falling in the rhombohedral structure except for one, ⟨0 0 4⟩ plane, hence it is concluded that the structure is hexagonal. The hexagonal structure of SnSb alloy is undisturbed due to the substitution of the transition metals Fe, Co and Ni. The XRD pattern of SnSb and SnSb:Ni samples indicate the presence of parental trace materials, namely Sn and Sb, similar to the one reported by Chaoli Yin et al. [11]. The absences of parent material in the substituted samples imply better structural stability.

The SEM micrographs of SnSb, SnSb:Fe, SnSb:Co and SnSb:Ni are shown in Fig. 2A–D, respectively. The SnSb (A) shows agglomerated particles of 100 nm size and SnSb:Fe (B), SnSb:Ni (D) shows the particle size of 60 nm with higher agglomeration than pure SnSb. It is to be noted that, SnSb:Ni (D) sample shows a very low particle size

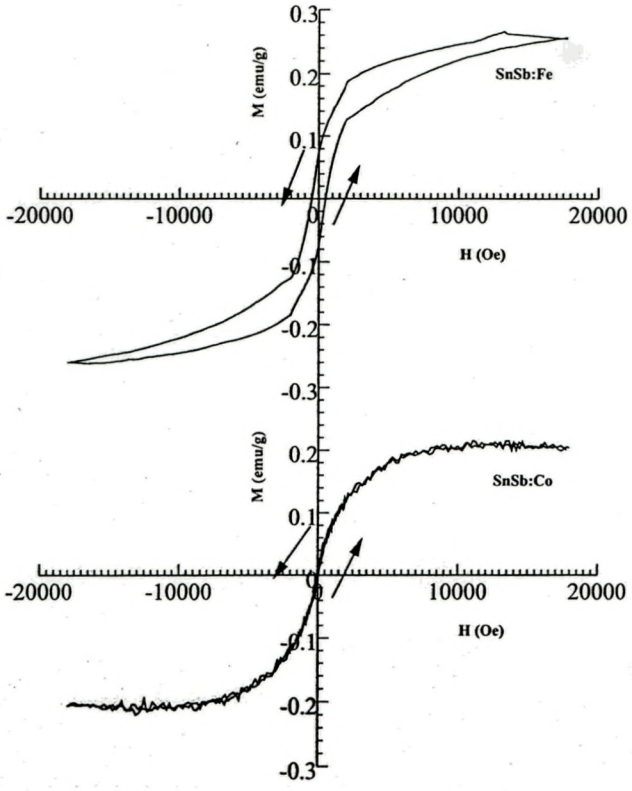

Fig. 4. VSM spectra for SnSb:Fe and SnSb:Co samples.

Table 1
Magnetic properties of samples SnSb:Fe and SnSb:Co.

Properties	SnSb:Fe	SnSb:Co
Hc (Oe)	500	45
Ms (emu/g)	0.256	0.205
Mr/Ms	0.297	0.243

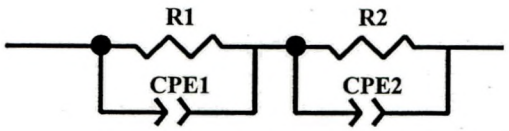

Fig. 5. Equivalent circuits for SnSb, SnSb:Fe, SnSb:Co and SnSb:Ni samples.

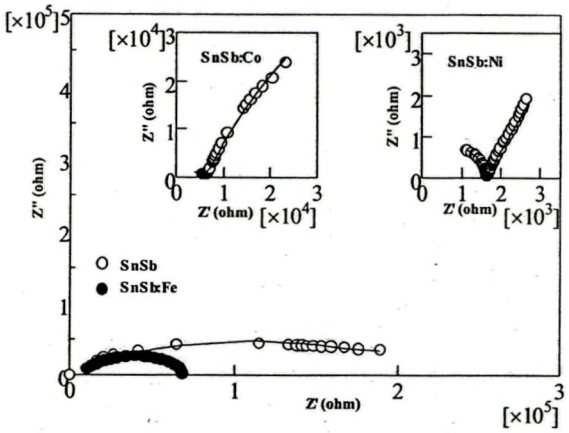

Fig. 6. Nyquist plots for SnSb, SnSb:Fe, SnSb:Co and SnSb:Ni samples.

than the reported one, by Guo et al., which is the only available literature, where the particle size of SnSb:Ni is 2–10 μm range and also the ratio of Sn in SnSb:Ni is higher than the present work [14]. In contrast, in the SnSb:Co (C) sample (Particle size 20 nm), very high agglomeration is observed than SnSb, SnSb:Fe and SnSb:Ni. The average particle size is calculated from several SEM micrographs obtained at different locations, however only one is shown in this article.

Compositional analysis of SnSb, SnSb:Fe, SnSb:Co and SnSb:Ni was carried out by EDX. A non-stoichiometric ratio of $Sn_{1.8}Sb_{2.94}$, $Fe_{0.95}Sn_{1.98}Sb_{3.07}$, $Co_{1.39}$ $Sn_{1.29}$ $Sb_{2.26}$ and $Ni_{0.97}Sn_{2.02}Sb_{3.01}$ is observed. It is not possible to comment on the stoichiometry of SnSb, as parent traces were observed in XRD. In the cobalt substitution, Co has entered the lattice and replaced antimony. It is noteworthy that Co metallic or oxide peaks are not seen in the XRD. Lattice strain due to cobalt inclusion has also been confirmed using FTIR and Raman analysis (spectra not given in this article).

The XPS spectra of SnSb and SnSb:Co are presented in Fig. 3(a–e) and the elements, Sn, Sb and Co are detected. The corresponding oxide peaks are also analyzed in the XPS spectra. The peaks obtained are curve fitted. Fig. 3(a and b) show peaks with binding energies 530.4, 530.2 eV corresponding to $3d^5$ of Sb and 540.2, 539.7 eV attributed to $3d^3$ of Sb in the pure and cobalt substituted alloys respectively. From the Fig. 3(c and d), the peaks observed at binding energies 486.8, 486.3 eV belongs to Sn–O and 495.3, 494.9 eV are attributed to 3d of Sn [15] are observed. No peak at 487.3 eV (SnO_2) is observed, indicating that the oxygen is only adsorbed on the surface and does not exist in a molecular bondage with Sn [15]. This is in conformation with the presence of water molecule through FTIR and Raman analysis. There is no major variation in binding energy shift due to the addition of transition metals. Fig. 3(e) show peaks with binding energies 781.5 and 797.9 eV corresponding to $Co(OH)_2$ and $2p^1$ of Co [15] respectively. The detected $Co(OH)_2$ peak reconfirms the ionization of adsorbed water molecule and creating charged surface on the nanoparticles of the alloy. The Co incorporation in SnSb does not alter the binding energies of $3d^3$ state of Sb and 3d state of Sn. Therefore it is concluded that the Co takes an intermediate positioning in the structure entangling both Sn and Sb with almost equal mutual forces thus making the structure more stable. Moreover, Co incorporated SnSb are magnetically characterized by vibrating sample magnetometer, in order to know the changes in the SnSb nanoalloy.

The SnSb and SnSb:Ni are diamagnetic as both the samples could not be magnetized no matter how much the heavy magnetic field is applied, whereas SnSb:Fe and SnSb:Co exhibit ferromagnetic behaviour. Houde et al. [16], reported that the magnetization curves of the Ni@Au nanoparticles exhibits superparamagnetic nature and Au@Ni nanoparticles show typical ferromagnetic nature at room-temperature and the drastic change in magnetization indicating that the majority element dominates in deciding the magnetic property. Hence in the present case, Fe and Co substitution resulted in ferromagnetic property while Ni substitution resulted in the diamagnetic nature that is of the SnSb itself. Fig. 4 shows the hysteresis curve of SnSb:Fe and SnSb:Co alloy nanoparticles. The magnetic properties of SnSb:Fe and SnSb:Co are listed in Table 1. The coercivity value of 500 Oe is measured for SnSb:Fe. The ferromagnetic hysteresis shows a saturation magnetization of 0.256 emu/g and 0.205 emu/g for SnSb:Fe and SnSb:Co, respectively and these values are slightly higher than the mass magnetization obtained in the $Ni_{43}Mn_{46}Sn_{11-x}Sb_x$ alloy, a popular soft magnet with Sn and Sb [5]. In contrary, Co-substitution results in nearly a superparamagnetic behaviour with saturation magnetization of 0.205 emu/g and coercivity of 45 Oe. The superparamagnetic nature of Co substituted SnSb sample of an abrupt reduction in magnetization can only be due to the particle size effect that is in good agreement with SEM results, as there is no change in oxidation state identified for Co through XPS results or any other binding probability

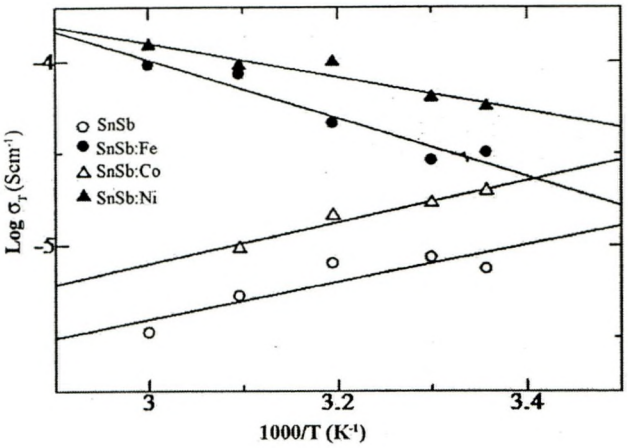

Fig. 7. Arrhenius plots for SnSb, SnSb:Fe, SnSb:Co and SnSb:Ni samples.

with Sn or Sb specifically through FTIR or Raman analysis. The XRD studies have also shown that there is no difference in the structure. The only reason for this drastic difference in the mass magnetization curve between SnSb:Co and SnSb:Fe samples would be only due to the varying antimony concentration setting pace of chemical kinetics in the crystallization process during the preparation of nanoparticles. Superparamagnetism can also be due to the highest concentration of Co in the SnSb:Co sample as supported by the EDX result.

Further studies for ac conductivity at varied temperatures are carried out. Fig. 6 shows the Nyquist plot (AC impedance spectra) for the SnSb, SnSb:Fe, SnSb:Co and SnSb:Ni alloy nanoparticles at 30 °C, respectively. The dots correspond to measured data and the line corresponds to theoretical fit. The entire spectrum has two semicircles and these semicircles can be attributed to the behaviour of bulk conductivity and grain boundary conductivity of the nanoparticles. The proposed equivalent circuit for both the samples is represented in Fig. 5, is (RQ) (RQ) [17,11] using the circuit description code. The total conductivity of SnSb increases after the addition of transition metals like Fe, Co and Ni from 8.576×10^{-6} S cm^{-1} to 2.903×10^{-5} S cm^{-1}. The Fe and Ni substitution exhibits the highest conductivity which indicates that all the other samples possessed severe electronic scattering resulting in reduced conductivity. As discussed above, this is an expected one as the excess of atoms available in the system could remain in the interstitial position causing electron scattering towards reduction in conductivity.

The Arrhenius plot for all samples at different temperatures from room temperature to 60 °C is shown in Fig. 7. The conductivity of Fe and Ni substituted SnSb sample increases with the increase in temperature. In contrast, the conductivity of pure SnSb and Co substituted SnSb sample decreases with the increase in temperature. Therefore, it is concluded that the SnSb:Fe and SnSb:Ni have thermally activated samples and SnSb and SnSb:Co is not activated thermally. The typical curves for SnSb:Fe and SnSb:Ni are linear, and the conductive behaviour of the sample follows the Arrhenius Eq. (1) in the measured temperature range.

$$\sigma = \sigma_0 \exp\left(\frac{-E_a}{RT}\right) \quad (1)$$

where σ is the ionic conductivity, σ_0, E_a, R, and T are the pre-exponential factor, the apparent activation energy, the gas constant, and the absolute temperature, respectively. The apparent activation energy of the pure SnSb sample got decreased to the minimal value of 0.08 eV when the particle size increases. In contrast, Fe, Co and Ni substituted SnSb shows an apparent activation energy of ≤0.1 eV and this result suggests that, the effect of reduction in particle size implies higher activation energy. Due to the incorporation of transition metal ion in the alloy lattice, a drastic change in conductivity from 8.576×10^{-6} to 2.903×10^{-5} S cm^{-1} has been realized even at 60 °C annexed with effect of magnetization say the superparamagnetism, which can be employed in any thermally activated magnetic application. However, this article does not cover the effect of magnetization at these temperatures and will be reported in the near future.

4. Conclusion

In this work, a new type of nanosized transition metals (Fe, Co and Ni) substituted SnSb alloy system has been synthesized by reductive co-precipitation method. Due to the addition of Fe, Co and Ni, no structural change occurs in the pure SnSb alloy. Th[illegible] Fe and Co substituted SnSb alloy show ferromagnetic properties while the SnSb and other substituted alloys exhibit diamagnetic properties. The Co substituted SnSb alloy exhibits superparamagnetic properties due to the effect of reduced particle size and not due to the oxidation states of any of the substituted elements in the alloy as observed from XPS results. From the conductivity studies, it can be clearly shown that conductivity of Fe and Ni substituted SnSb increases by one order of magnitude than the other samples.

References

[1] H. Gleiter, Mater. Sci. Eng. 52 (1982) 91–131.
[2] Z.H. Zhou, J.M. Xue, H.S.O. Chan, J. Wang, Mater. Chem. Phys. 75 (2002) 181–185.
[3] F. Heringhaus, T.A. Painter, Mater. Lett. 57 (2002) 787–793.
[4] F.X. Liu, T.Z. Li, Mater. Lett. 59 (2005) 194–196.
[5] T. Krenke, M. Acet, E.F. Wassermann, X. Moya, L. Manosa, A. Planes, Phys. Rev. 72 (2005) 014–412.
[6] Z.D. Han, D.H. Wang, C.L. Zhang, B.X. Gu, Y.W. Du, Appl. Phys. Lett. 90 (2007) 042507.
[7] M. Khan, I. Dubenki, S. Stadler, N. Ali, J. Phys.: Condens. Matter 16 (2004) 5259–5266.
[8] Z. Wang, T. Wenhuai, L. Xingguo, J. Alloys Compd. 439 (2007) 350–354.
[9] F. Wang, M. Zhao, X. Song, J. Alloys Compd. 472 (2009) 55–58.
[10] Z. Wanga, W. Tianc, X. Liud, R. Yanga, X. Lia, J. Solid-State Chem. 180 (2007) 3360–3365.
[11] C. Yin, H. Zhao, H. Guo, X. Huang, W. Qiu, J. Univ. Sci. Technol. Beijing 14 (2007) 345–349.
[12] B.H. Lee, Y.D. Kim, K.H. Lee, Biomaterials 24 (2003) 2257–2266.
[13] M.S. Park, S.A. Needham, G.X. Wang, Y.M. Kang, J.S. Park, S.X. Dou, H.K. Liu, Chem. Mater. 19 (2007) 2406–2410.
[14] H. Guo, H. Zhao, X. Jia, W. Qiu, F. Cui, Mater. Res. Bull. 42 (2007) 836–843.
[15] F. Sheng Ke, L. Huang, B.C. Solomon, G.Z. Wei, L.J. Xue, B. Zhang, J.T. Li, X.D. Zhou, S.G. Sun, J. Mater. Chem. 34 (2012) 17511–17517.
[16] S. Houde, Y. Chen, X. Chen, K. Zhang, Z. Wang, D.L. Peng, J. Mater. Chem. 22 (2012) 2757–2765.
[17] H. Mukaibo, T. Osaka, P. Reale, S. Panero, B. Scrosati, M. Wachtler, J. Power Sources 132 (2004) 225–228.